

MIT Open Access Articles

*Probing plasma turbulence by modulating
the electron temperature gradient*

The MIT Faculty has made this article openly available. **Please share** how this access benefits you. Your story matters.

Citation: DeBoo, J. C. et al. "Probing plasma turbulence by modulating the electron temperature gradient." *Physics of Plasmas* 17 (2010): 056105. © 2010 American Institute of Physics.

As Published: <http://dx.doi.org/10.1063/1.3316298>

Publisher: American Institute of Physics

Persistent URL: <http://hdl.handle.net/1721.1/67332>

Version: Final published version: final published article, as it appeared in a journal, conference proceedings, or other formally published context

Terms of Use: Article is made available in accordance with the publisher's policy and may be subject to US copyright law. Please refer to the publisher's site for terms of use.



Probing plasma turbulence by modulating the electron temperature gradient^{a)}

J. C. DeBoo,^{1,b)} C. Holland,² T. L. Rhodes,³ L. Schmitz,³ G. Wang,³ A. E. White,^{4,c)} M. E. Austin,⁵ E. J. Doyle,³ J. Hillesheim,³ W. A. Peebles,³ C. C. Petty,¹ Z. Yan,⁶ and L. Zeng³

¹General Atomics, P.O. Box 85608, San Diego, California 92186-5608, USA

²University of California-San Diego, 9500 Gilman Drive, La Jolla, California 92093, USA

³University of California-Los Angeles, 405 Hilgard Avenue, Los Angeles, California 90095, USA

⁴Oak Ridge Institute for Science and Education, 130 Badger Avenue, Oak Ridge, Tennessee 37830-6218, USA

⁵University of Texas-Austin, P.O. Box 8028, Austin, Texas 78713, USA

⁶University of Wisconsin at Madison, 337 Engineering Research Building, 1500 Engineering Drive, Madison, Wisconsin 53706, USA

(Received 21 November 2009; accepted 22 January 2010; published online 15 March 2010)

The local value of a/L_{Te} , a turbulence drive term, was modulated with electron cyclotron heating in L-mode discharges on DIII-D [J. L. Luxon, Nucl. Fusion **42**, 614 (2002)] and the density and electron temperature fluctuations in low, intermediate, and high- k regimes were measured and compared with nonlinear gyrokinetic turbulence simulations using the GYRO code [J. Candy and R. E. Waltz, J. Comput. Phys. **186**, 545 (2003)]. The local drive term at $\rho \sim 0.6$ was reduced by up to 50%, which produced comparable reductions in electron temperature fluctuations at low- k . At intermediate k , $k_\theta \sim 4 \text{ cm}^{-1}$ and $k_\theta \rho_s \sim 0.8$, a very interesting and unexpected result was observed where density fluctuations increased by up to 10% when the local drive term was decreased by 50%. Initial comparisons of simulations from GYRO with the thermal diffusivity from power balance analysis and measured turbulence response are reported. Simulations for the case with the lowest drive term are challenging as they are near the marginal value of a/L_{Te} for trapped electron mode activity. © 2010 American Institute of Physics. [doi:10.1063/1.3316298]

I. INTRODUCTION

Validating transport models based on the gyrokinetic model of plasma microturbulence by careful comparison of turbulence and transport simulations with experimental measurements is an essential step toward accurate predictive capability of plasma transport in tokamak plasmas. Such a validated model will serve an essential function in the design and understanding of experiments in the next generation of tokamak devices with fusion-grade plasmas such as ITER.¹ Experiments with a single key parameter varied and the turbulence response measured provide excellent data sets for model validation studies. This paper describes the results of one such experiment on DIII-D (Ref. 2) where the electron temperature gradient and thus gradient scale length was systematically varied and the turbulence response across a wide wave number range documented, including both density and temperature fluctuations. Initial comparison of some of the results with simulations from the GYRO (Ref. 3) code, which computes nonlinear turbulence and transport coefficients, is also discussed.

Previous experiments have been performed where the emphasis was on characterizing and comparing electron mode turbulence with simulations. In experiments on DIII-D

electron cyclotron heating (ECH) power was utilized to increase the electron temperature and correlate profile changes with enhanced turbulence.^{4,5} On Alcator C-Mod⁶ nonlinear simulations reproduced the relative increase in trapped electron mode (TEM) fluctuations measured when on-axis ion cyclotron resonance heating power was applied.⁷ The experiments reported here held auxiliary power fixed while varying the local TEM turbulence by varying the local ∇T_e at roughly fixed electron and ion temperature and density.

The motivation for the experiment was to test nonlinear gyrokinetic turbulence simulations against measurements from a controlled experiment, emphasizing both qualitative and quantitative comparisons. We chose to emphasize electron transport where smaller size turbulent eddies play a key role. Thus plasma parameters and profiles were chosen where linear analysis indicated that ion temperature gradient (ITG) modes at low wave number k were subdominant in order to emphasize the impact of TEMs at low and intermediate- k and possibly electron temperature gradient (ETG) modes at high- k . It was intended that this choice would also help to simplify the comparison between experiment and simulation by isolating a drive term for a single key driftwave, TEMs, in order to test the key physics in the code for this mode.

The experimental approach was to produce local, controlled, and reproducible changes in ∇T_e and thus in the inverse temperature gradient scale length $1/L_{Te} = |\nabla T_e|/T_e$, a drive term for TEM activity, using ECH. The inverse tem-

^{a)}Paper KI3 3, Bull. Am. Phys. Soc. **54**, 138 (2009).

^{b)}Invited speaker.

^{c)}Current address: Massachusetts Institute of Technology, Cambridge, Massachusetts 02139, USA.

perature gradient scale, a/L_{Te} (where the normalization factor a is the plasma minor radius) was modulated repetitively during individual discharges and the response of turbulence activity across ITG, TEM, and ETG scales was documented in order to compare the measured response with code simulations. In response to changes in a/L_{Te} , changes in turbulence activity were observed at all turbulence scales from low to high wave numbers but the most interesting response occurred at intermediate wave numbers. The response to moderate changes in drive term was generally as expected based on linear theory: decreasing the drive term resulted in decreased low- k T_e fluctuations and intermediate- k density fluctuations. However, a very interesting change in response at intermediate- k was observed for density fluctuations when the drive term was further reduced by up to 50%. While low- k T_e fluctuations were further reduced, the intermediate- k density fluctuation response reversed, increasing when the drive term decreased. This is a clear challenge to linear stability theory and remains to be seen whether the observation can be understood with nonlinear theory. Generally the experiment has yielded an excellent data set for nonlinear gyrokinetic turbulence code validation studies, where not only trends in the turbulence but quantitative comparisons with simulations can be made. This paper describes the experimental results and reports on just a few of the many detailed comparisons between simulations and measurements that can be carried out.

II. EXPERIMENTAL CONDITIONS

The target discharge for these experiments was an L-mode discharge limited against the inside wall of the vacuum vessel in order to inhibit an L–H-mode transition and subsequent transient events such as edge localized modes. To further avoid transients associated with magneto-hydrodynamic activity the plasmas studied were at low plasma pressure, toroidal beta $\sim 0.2\%$, and low current, 0.8 MA, with ECH being the only auxiliary heating during the flattop phase of the plasma current. Line averaged electron density was feedback controlled to low values, $2 \times 10^{19} \text{ m}^{-3}$, in order to maintain low collisionality which favors TEM-scale turbulence over longer wavelength ITG activity. During the time when ECH was applied, for 4 s during the steady-state phase of the plasma current, small sawteeth were present with a normalized inversion radius of $\rho \sim 0.25$, which typically did not impact turbulence measurements in the outer half of the plasma.

The ECH system comprises up to six gyrotrons at 110 GHz with waves launched radially into the plasma in X-mode polarization to maximize the single pass absorption at the second harmonic resonant layer. Power was resonant at two closely spaced positions in the plasma [Fig. 1(a)]. For the first 2 s during the steady-state phase of the plasma current, four gyrotrons were employed, two at each location, and for the following 2 s six gyrotrons were employed, three at each location, to further increase the change in local a/L_{Te} . ECH power from each pair or triplet was alternately applied in 25 ms intervals so as to modulate ∇T_e and gradient scale length between the two deposition peaks at a

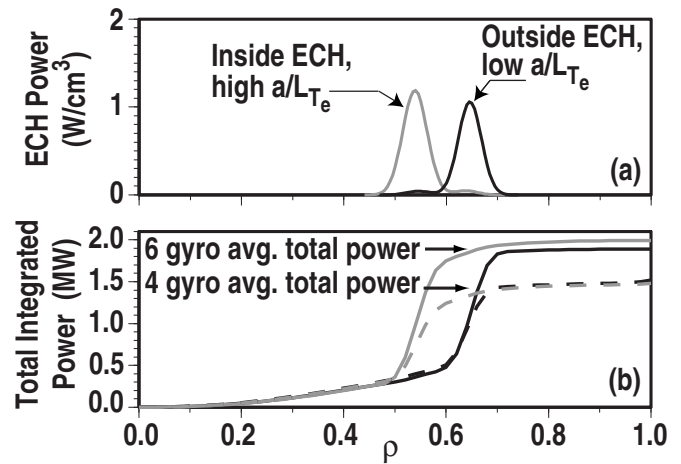


FIG. 1. (a) ECH power density for inside heating producing high a/L_{Te} at $\rho \sim 0.6$ and outside heating producing low a/L_{Te} . (b) Ohmic+ECH integrated power for six gyrotrons [solid gray (inside ECH) and black (outside ECH) lines] and four gyrotrons (dashed).

roughly constant value of the midpoint T_e . The combined peak power for each pair and triplet was matched to within 100 kW or less at ~ 0.9 and ~ 1.4 MW, respectively, so that power to the plasma remained constant as the heating location was modulated from just inside (inside ECH) to outside (outside ECH) the region of interest. Total heating power, ECH plus Ohmic, for the four and six gyrotron phases was ~ 1.5 and 2 MW, respectively [Fig. 1(b)]. The region of interest was chosen to be where linear stability analysis indicated TEM growth rates were most dominant over ITG growth rates, $\rho_{ECH} = 0.5, 0.6, \text{ and } 0.7$. The focus of the results presented in this paper is at $\rho_{ECH} = 0.6$ with comments on other locations when the results differed significantly. The power duty cycle of each gyrotron pair was 90% of peak power. This resulted in a power deposition profile with a main peak at one location and a smaller peak at the other location as seen in Fig. 1(a). The main peaks were spatially separated by approximately 5 cm and thus turbulence diagnostics with good spatial resolution ($\Delta r \leq 1$ cm) were key to the experiment.

The linear stability analysis referred to above and throughout this paper was performed with the TGLF (Ref. 8) code. Growth rates were computed over the range $k_{\theta}\rho_s = 0.01 - 80$. The sign of the real frequency was generally used to distinguish ITG from TEM dominated activity. This choice was further supported by the result that reducing a/L_{Te} by 50% changed the calculated maximum growth rates by 15% or less over the spectral region where the real frequency indicated TEM domination for the high drive term condition. TEM mode growth rates are calculated to dominate ITG modes typically over the range $k_{\theta}\rho_s > 0.2$ for the high drive term state. When a/L_{Te} is reduced by up to 50% the region of TEM dominance moves to slightly larger values, $k_{\theta}\rho_s > 0.4$.

As a result of constant ECH power applied during inside and outside ECH phases the density and ion temperature profiles remained constant [Figs. 2(a)–2(c)]. As seen in Figs. 2(d)–2(f) the impact of six versus four gyrotrons also did not change the density and ion temperature profiles and raised T_e

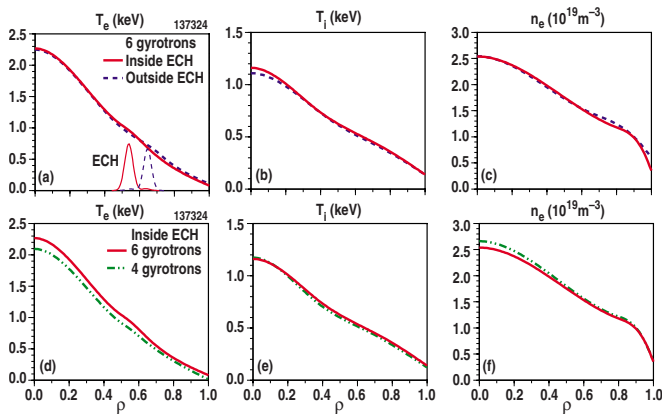


FIG. 2. (Color online) Profiles (a–c) for six gyrotron case with inside (solid) and outside (dashed) ECH and (d–e) for inside ECH with six gyrotrons (solid) and four gyrotrons (dash-dot-dot).

about 15% so that small changes in the ratio of T_e/T_i accompanied six versus four gyrotron operation. However, the largest impact on turbulence was due to changes produced in the local temperature gradient scale length based on linear analysis with the TGLF code. The ratio of T_e/T_i was about 2. An intermediate density gradient favored electron driftwave mode activity. Neutral beam blips, 2 ms in duration every 225 ms, were employed to make ion temperature, plasma rotation, and impurity density measurements with a charge exchange recombination diagnostic. Due to negligible torque from the neutral beam blips, plasma rotation was very small. Simulations for the case with $\rho_{\text{ECH}}=0.5$ with and without $E \times B$ shear included showed that $E \times B$ stabilization effects were negligible. Z_{eff} was between 2.5 and 3 for these low density plasmas with carbon being the dominant impurity. The dominant power loss was by thermal conduction for both the electrons and ions based on analysis with ONETWO (Ref. 9) while the major power input was 1.5 MW of ECH for electrons and about 200 kW for the ions from collisional transfer of energy from electrons. The calculated power loss due to neoclassical ion diffusion was small over most of the plasma and only comparable to the input power at the plasma center.

III. MODULATION OF a/L_{T_e}

The local value of a/L_{T_e} was significantly varied by spatially modulating the ECH. Local values of a/L_{T_e} were computed with the electron cyclotron emission (ECE) diagnostic¹⁰ system. In order to reduce noise associated with calculating spatial gradients, the ECE channels were first phase lock averaged over 19 ECH periods, a total of 950 ms to obtain local values of T_e during both four and six gyrotron heating phases in the discharge, and then ∇T_e was computed by differencing adjacent ECE channels. The phase lock averaged local values of T_e from a single discharge are shown in Fig. 3(a) for the four gyrotron heating phase with the location of the maximum change in a/L_{T_e} indicated at $\rho=0.62$. The shot to shot reproducibility of a/L_{T_e} was very good as can be seen in Fig. 3(b) where the phase lock averaged time history of several repeat shots are shown over the

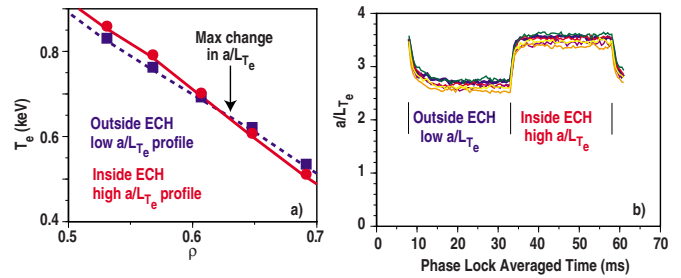


FIG. 3. (Color online) (a) Electron temperature profiles from ECE for inside (solid) and outside (dashed) ECH. Profiles have been phase lock averaged over 19 ECH periods of 50 ms each. (b) Variation of normalized inverse temperature gradient scale length with time during inside and outside ECH determined by differencing adjacent ECE channels for multiple discharges.

duration of an ECH period. The figure also shows that a/L_{T_e} is quite constant during each phase and achieved a new equilibrium rapidly (in less than 5 ms) following a change in ECH deposition location.

A reduction in a/L_{T_e} of up to 25% was achieved with four gyrotrons and later in the same discharges the reduction was increased to 50% with six gyrotrons (Fig. 4). The change in a/L_{T_e} is referenced to the profile condition with inside ECH, the high a/L_{T_e} , or high TEM drive, phase. The largest change in a/L_{T_e} is spatially localized to the region between inside and outside ECH deposition peaks. There is a much smaller increase in a/L_{T_e} near $\rho \sim 0.45$, which corresponds to the region just inside of the deposition peak for inside ECH where ∇T_e is flattened and then returns to a steeper value when inside ECH is removed. The location of the largest decrease in a/L_{T_e} moves slightly outward for six versus four gyrotrons, from $\rho=0.62$ to 0.66, which may be a result of the deposition of the additional two gyrotrons not exactly matching that of the four gyrotrons.

The experimental T_e profiles shown in Fig. 2 exceed the marginal stability condition for electron modes at intermediate wave numbers in the region where ECH is applied during the high a/L_{T_e} phase based on linear stability analysis with TGLF and approach the marginal condition when a/L_{T_e} is reduced. Figure 5(a), which is for the inside ECH case with four gyrotrons, indicates the marginally stable condition is at $a/L_{T_e} \sim 2$ where the normalized growth rates change slope for normalized wave numbers $k_{\theta}\rho_s \geq 0.5$ and increase more

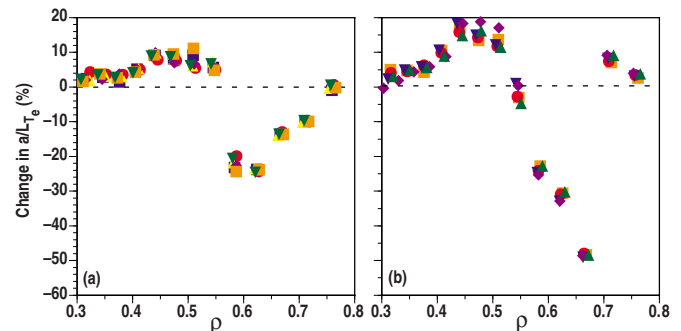


FIG. 4. (Color online) Change in drive term for (a) four gyrotron and (b) six gyrotron cases for multiple discharges. The reference for determining the change in drive term is the high a/L_{T_e} (inside ECH) phase.

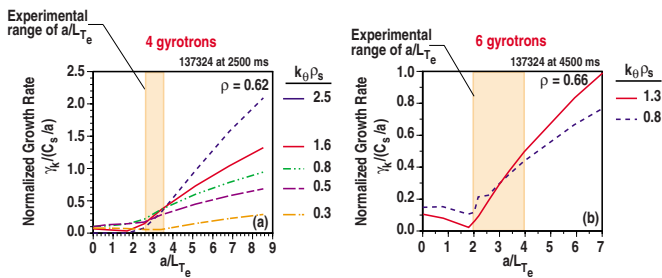


FIG. 5. (Color online) Marginality condition based on linear analysis for (a) four gyrotron and (b) six gyrotron cases. The experimental range in drive term a/L_{Te} is displayed by the shaded region. The six gyrotron case is at the marginal stability condition $a/L_{Te} \sim 2$ during the low a/L_{Te} phase.

rapidly with a/L_{Te} . The experimental value of a/L_{Te} is above the marginal value indicating electron mode turbulence is active. When the value of a/L_{Te} is reduced by applying outside ECH the curves in Fig. 5 indicate the growth rates should then decrease, which is consistent with our observations with four gyrotrons. It is interesting to note that the curves also indicate that the largest change in growth rate occurs for larger values of $k_\theta \rho_s$, emphasizing intermediate- k values is where one should expect the largest changes to occur compared with lower- k values, $k_\theta \rho_s \leq 0.3$ where no marginal condition exists. For the lowest values of a/L_{Te} produced, the case with six gyrotrons, linear analysis indicates that during the low a/L_{Te} phase [left border of shaded region in Fig. 5(b)] the plasma is at the marginal condition where there is a transition from ∇T_e driven to ∇n_e driven electron modes with small increases in growth rate occurring below the transition. Below the marginal condition the real frequency of the modes is positive indicating electron modes. However, the growth rate is somewhat sensitive to variation in a/L_{Ti} , increasing a factor of 2 when a/L_{Ti} is decreased by 50%.

IV. TURBULENCE RESPONSE

DIII-D has an excellent set of turbulence diagnostics with good spatial resolution and full coverage of driftwave spectra from low to high wave number. Low- k , ITG and TEM scale, density fluctuations were monitored with a two-channel Doppler backscattering system¹¹ (DBS2) with a spatial resolution of $\Delta r \sim 1$ cm and for a few special shots with neutral beam power added, a beam emission spectroscopy (BES) system¹² with a radial resolution $\Delta r \sim 0.8$ cm. Temperature fluctuations at low- k were monitored with a correlation electron cyclotron emission (CECE) system¹³ with a spatial resolution of 0.5 cm. Intermediate- k , TEM scale, density fluctuations were monitored with a five-channel Doppler backscattering system¹⁴ (DBS5) with a spatial resolution of $\Delta r \sim 1$ cm. High- k , ETG scale, density fluctuations were monitored with a millimeter-wave backscattering system¹⁵ (HKBS) with a much broader spatial response, $\Delta r \sim 25$ cm covering the plasma region $\rho = 0.6 - 1.0$.

Turbulence at intermediate- k provided the most interesting and surprising change in response for four versus six gyrotrons. The amplitude of poloidal density fluctuations measured at $k_\theta \sim 4$ cm⁻¹ with DBS5 was positively corre-

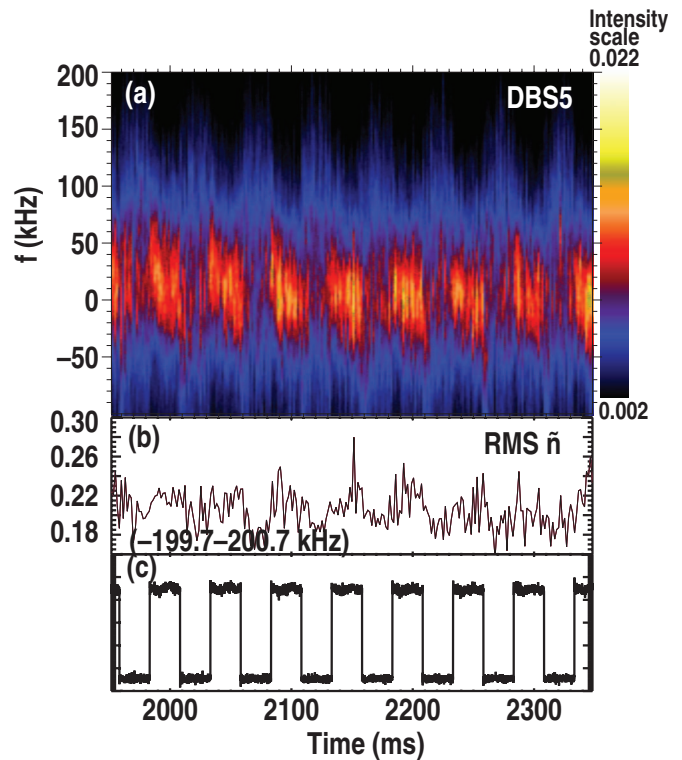


FIG. 6. (Color) (a) Spectral contour plot with color indicating amplitude and (b) rms density fluctuations for the DBS5 measuring intermediate- k density fluctuations. (c) Indication of high a/L_{Te} periods of time.

lated with changes in the drive term a/L_{Te} during the four-gyrotron phase of the discharges. Figure 6(a) displays the spectral contour plot of frequency versus time with color denoting amplitude variations. As expected based on linear theory the fluctuation amplitude decreased when the drive term decreased and increased when the drive term increased as illustrated in Fig. 6(b) where the rms fluctuation amplitude integrated over frequency is shown. The frequency is also modulated somewhat but is not likely due to changes in the turbulence but rather presumed to be due to changes in the plasma poloidal rotation velocity, which were too small to be measured. DBS measures the laboratory frame backscattered frequency, which is determined by the Doppler-shifted turbulence frequency as $\omega_{DBS} = \omega_i + k_\theta v_{ph} + \mathbf{k}_\theta \times \mathbf{v}_{E \times B}$ where ω_i is the incident probing frequency. Thus the measured backscattered frequency has contributions from both the turbulence phase velocity v_{ph} and poloidal velocity associated with $E \times B$ motion. However, nonlinear calculations from GYRO show that both the magnitude and the change in $k_\theta v_{ph}$ are small compared to the change in laboratory frame frequency observed, $\Delta f_{DBS} \sim 20 - 30$ kHz [Fig. 6(a)]. This suggests that the change in frequency observed is dominated by Doppler shifts associated with poloidal $E \times B$ motion (which is small enough to have no impact on turbulence stabilization by $E \times B$ flow shear).

A spatial scan of the DBS5 system was performed over several shots to determine the spatial profile of the turbulence response. In order to reduce the amplitude uncertainty the signals were integrated over all frequency and phase lock averaged over 19 ECH periods, 950 ms, and then the differ-

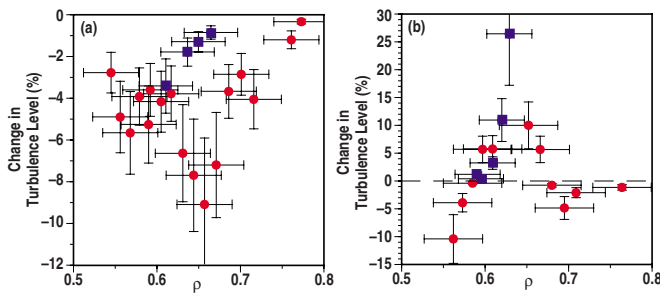


FIG. 7. (Color online) Magnitude and spatial distribution of the change in intermediate- k density fluctuations for (a) four gyrotrons and (b) six gyrotrons for $k_\theta \sim 4 \text{ cm}^{-1}$ (circle) and $\sim 8 \text{ cm}^{-1}$ (square).

ence in signals during low and high a/L_{Te} phases was normalized to the high a/L_{Te} phase to determine the change in turbulence level relative to the high a/L_{Te} phase for both the four and six gyrotron heating phases (Fig. 7). The multishot spatial scan was performed with the system measuring $k_\theta \sim 4 \text{ cm}^{-1}$. The response at this wave number shows that the change in turbulence was spatially localized to the region where the drive term was modulated and for four gyrotrons the intermediate- k turbulence amplitude decreased by up to 10% [Fig. 7(a)] when the drive term was decreased by up to 25% [Fig. 4(a)]. A similar response was observed in a previous experiment with the ECH resonant at $\rho_{ECH}=0.5$ with a slightly larger turbulence response, decreasing by up to 17% for a drive term reduction of 30%. One additional shot with $\rho_{ECH}=0.6$ was taken with the system measuring $k_\theta \sim 8 \text{ cm}^{-1}$, the largest wave number possible with DBS5 for the experimental conditions, which shows a weaker response that appears slightly shifted radially. However, without additional shots to determine the spatial profile of the response at this wave number the result remains an interesting anomaly and motivation for future work.

The intermediate- k \tilde{n} response in the six gyrotron case was quite surprising, showing an inverse correlation with the change in drive term, increasing when the drive term decreased [Fig. 7(b)]. With six gyrotrons the drive term was reduced by up to 50% at $\rho=0.66$ and the turbulence at $k_\theta \sim 4 \text{ cm}^{-1}$ increased up to 10% and up to 25% or possibly higher at $k_\theta \sim 8 \text{ cm}^{-1}$. At smaller radii, $\rho=0.45-0.5$ beyond the peak in inside ECH deposition, the change in drive term was positive and apparently large enough to produce a change in turbulence activity in this region. We interpret the increase in density fluctuations at $\rho=0.56$ as due to the positive change in drive term at slightly smaller radii. The measurements did not extend to sufficiently small radii to document the turbulence response returning toward zero as does the change in drive term. Throughout the entire region measured, however, the turbulence response is inversely correlated with the change in a/L_{Te} . This behavior is a challenge to linear theory (i.e., Fig. 5 shows that a decrease in a/L_{Te} should result in a decrease in growth rate for a drive term above the marginal value of a/L_{Te}) and remains to be seen whether it can be understood with nonlinear theory. It is also interesting to note that the turbulence at $k_\theta \sim 4 \text{ cm}^{-1}$ further out in the plasma with $\rho_{ECH}=0.7$ had no response within

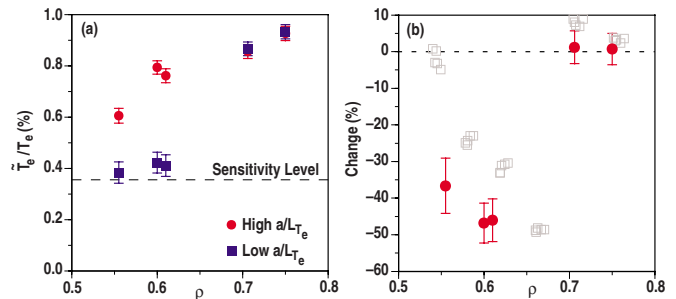


FIG. 8. (Color online) Low- k electron temperature fluctuation level (a) for the high (circle) and low (square) a/L_{Te} phases. (b) Magnitude and spatial distribution of change in electron temperature fluctuations (circle) and change in drive term (square).

experimental uncertainties to a decrease in drive term by 50%.

Long wavelength, low- k turbulent activity is particularly important to understand since the dominant contributions to heat flux and transport are usually due to this region of the turbulent spectrum¹⁶ (also see simulation results in this paper). In contrast to the density turbulence response at intermediate- k with $\rho_{ECH}=0.6$, there was no measurable change in low- k density fluctuations, $k_\theta \leq 2 \text{ cm}^{-1}$, with a 50% decrease in a/L_{Te} . The lack of response of low- k density fluctuations to the addition of ECH has been seen in other L-mode electron cyclotron heated plasmas.⁵ There was, however, a reduction in low- k temperature fluctuations measured with the CECE system which is sensitive to $k_\theta \leq 2 \text{ cm}^{-1}$. Fluctuations of $\tilde{T}_e/T_e \sim 0.4\% - 0.9\%$ were observed with six gyrotrons [Fig. 8(a)]. The relative change in \tilde{T}_e/T_e was comparable to the relative change in a/L_{Te} , up to $\sim 50\%$ decrease in \tilde{T}_e/T_e for a 50% decrease in a/L_{Te} [Fig. 8(b)]. These changes in turbulence amplitude occur for frequencies below $\sim 25 \text{ kHz}$. The CECE signals were also phase lock averaged over 19 ECH periods to reduce the uncertainty. Even with phase lock averaging changes in the temperature fluctuations were difficult to observe with a 25% reduction in a/L_{Te} with four gyrotrons as the signal size was approaching the noise level.

Another useful validation study comparison with code simulations that can be carried out is the relative phase between density and temperature fluctuations. The phase between temperature fluctuations and potential fluctuations and between density fluctuations and potential fluctuations are more fundamental to turbulent transport, but lacking these measurements the cross phase between density and temperature fluctuations is a useful comparison providing additional constraints on model simulations. These measurements were accomplished with the DBS2 and CECE systems coupled together to share plasma-viewing optics. The overlapping spatial volumes in the plasma allow simultaneous measurements of low- k density and temperature fluctuations and the cross-phase angle between them. The cross-phase angle was measured to be $80^\circ - 120^\circ$ in the frequency range 10–25 kHz. Measurements were made out to several hundred kilohertz but the cross-phase spectral response was found to be limited to frequencies below $\sim 30 \text{ kHz}$, similar to the frequency

range of low- k density and electron temperature fluctuations in these low rotation plasmas. It should be noted that only the six gyrotron, high a/L_{Te} case had a high enough coherency for a meaningful phase angle measurement.

High- k , ETG-scale, density fluctuations at $k_r \sim 35 \text{ cm}^{-1}$ showed a small inverse correlation with changes in a/L_{Te} where the turbulence level increased $\sim 10\%$ when a/L_{Te} decreased by 50%. Only after phase lock averaging the data over 19 ECH periods was this small change clearly observable. It is speculated, however, that this inverse correlation may be the result of the broad spatial resolution of the HKBS system rather than a result due to local changes in a/L_{Te} at $\rho \sim 0.6$. The spatial resolution is much broader than the other turbulence diagnostics employed in these experiments, covering a normalized plasma radius of $\rho \sim 0.6-1.0$ or about the outer 25 cm of the plasma. Since the HKBS system is sensitive to the edge where the ETG growth rates are calculated to be much larger than at $\rho=0.6$, based on linear analysis with TGLF, and the growth rates are sensitive to the ratio T_e/T_i the measurement may be more sensitive to small changes in T_e/T_i , produced by outside versus inside ECH, than to local changes in a/L_{Te} at $\rho=0.6$.

One final regime of interest probed in these experiments was a regime where the level of low- k ITG-scale activity was raised in the plasma by the addition of 2 MW of neutral beam heating. For this case T_i and T_e are more similar than without neutral beam injection (NBI). Linear analysis with TGLF indicates that the dominant growth rates are still electron modes for $k_{\theta}\rho_s \geq 0.4$. The addition of NBI afforded additional low- k density fluctuation measurements with the BES system which showed a change in low- k density turbulence for both four and six-gyrotron operations (Fig. 9) that was very similar to the change in a/L_{Te} in magnitude and spatial extent over the region measured. The full spatial extent of the change in turbulence was not measured but the peak in the response is clearly visible. This system includes a 5 radial \times 6 poloidal array of detectors scanned radially using two shots to construct the spatial profile shown in Fig. 9. The signals were phase lock averaged over 19 ECH periods, which reduced the measurement uncertainties and more importantly mitigated the impact of sawteeth, which increased in amplitude with the addition of NBI. The change in a/L_{Te} achieved in this case was reduced considerably compared to the ECH only cases because of the background heat flux from NBI, which effectively reduced the local change in total heat flux produced with ECH. Thus generally a weaker turbulence response compared to the response without NBI was observed due to a weaker change in drive term. In addition to the response of low- k density fluctuations monitored with BES, there was a different intermediate- k density turbulence response (from DBS5 measurements) with NBI compared to without NBI. For the case with a stronger change in drive term, with six gyrotrons with NBI, there was not only no reversal in the turbulence response observed but essentially little or no response to the change in drive term. This result is similar to observations at $\rho_{ECH}=0.7$ where for an $\sim 50\%$ decrease in a/L_{Te} there was also little or no change seen in intermediate- k density fluctuations.

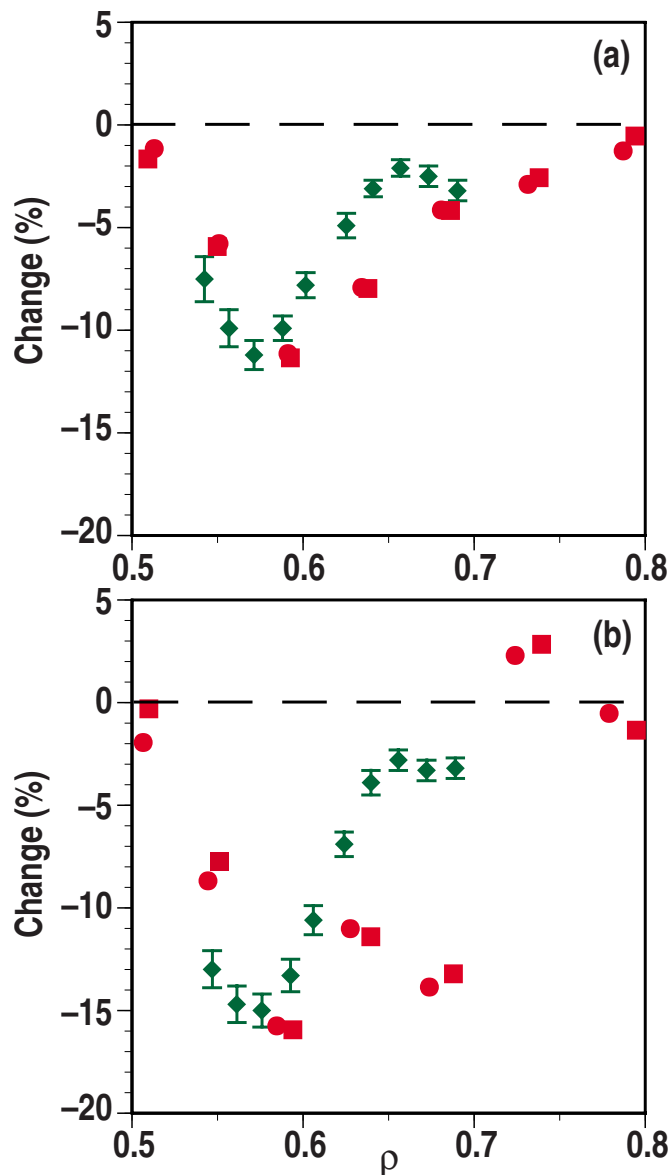


FIG. 9. (Color online) Change in low- k density fluctuations (diamond) and drive term (circle and square) for the special discharges with NBI for (a) four gyrotrons and (b) six gyrotrons.

V. SIMULATION COMPARISONS WITH MEASUREMENTS

Initial tests of turbulence code simulations are usually at the level of comparing heat flux simulations with experimental results from a power balance analysis. One typically would like to achieve a reasonable level of success at this level of comparison before continuing to the next more fundamental level of comparison with turbulence characteristics. Often detailed experimental information of the turbulence is not available. However with the results of these experiments one can perform unique comparisons of turbulence characteristics in specific spectral regimes. Each of the turbulence responses discussed above in three different wave number regimes can be used as a case study for comparison with results from simulations with nonlinear gyrokinetic turbulence codes such as GYRO. These types of comparisons have

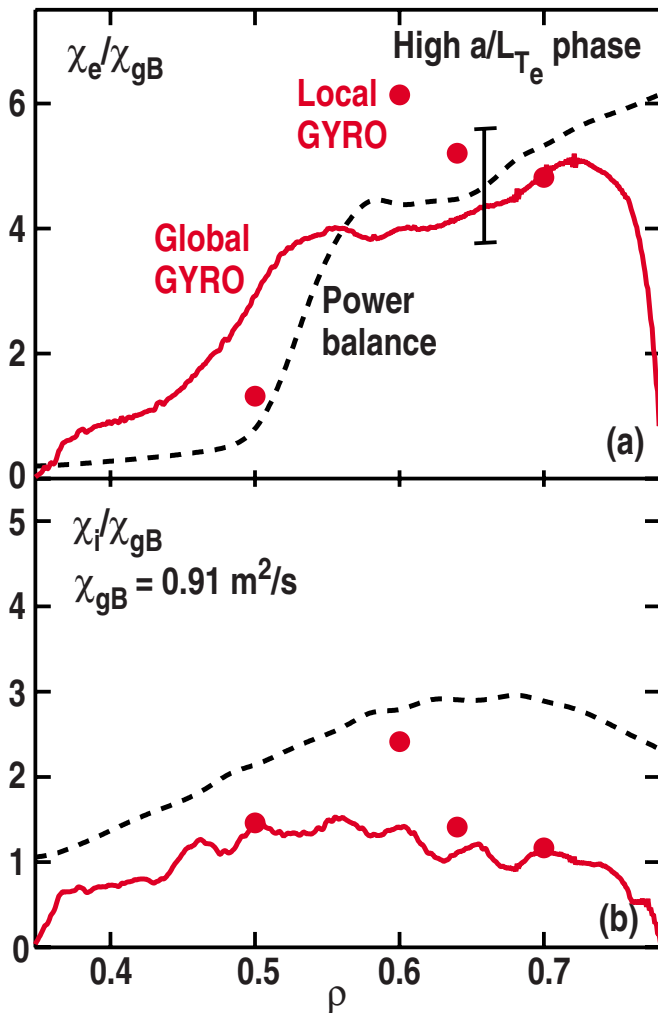


FIG. 10. (Color online) (a) Electron and (b) ion thermal diffusivities normalized to the gyroBohm diffusivity determined from power balance analysis (dashed line), a global GYRO simulation (solid), and local flux tube GYRO simulations (circle). The error bar shown represents the standard deviation of a distribution of 66 thermal diffusivities at $\rho=0.66$ determined by randomly varying input profile data within measurement uncertainties, refitting each perturbed profile and rerunning the power balance analysis with each set of perturbed profiles.

just begun for this experiment and thus only the first of many possible comparisons are reported here.

For the plasmas discussed in this paper there has been mixed success comparing heat flux and thermal diffusivity simulations with power balance analysis. Global and local flux tube simulations of electron thermal diffusivities from GYRO were found to be in reasonable agreement with calculations from a power balance analysis with ONETWO for the case with ECH at $\rho_{ECH}=0.6$. The GYRO simulations include the physics from electron collisions, plasma impurities, electromagnetic effects with reduced mass ratio $\mu=(m_i/m_e)^{1/2}=40$, and normalized wave numbers up to $k_{\theta}\rho_s \sim 2.5$. The global simulations, covering a wider plasma region than local flux tube simulations, are generally in reasonable agreement with local simulations for the high a/L_{Te} case (Fig. 10) for both electron and ion thermal diffusivities near the region where the maximum change in a/L_{Te} occurred, $\rho \sim 0.66$. The

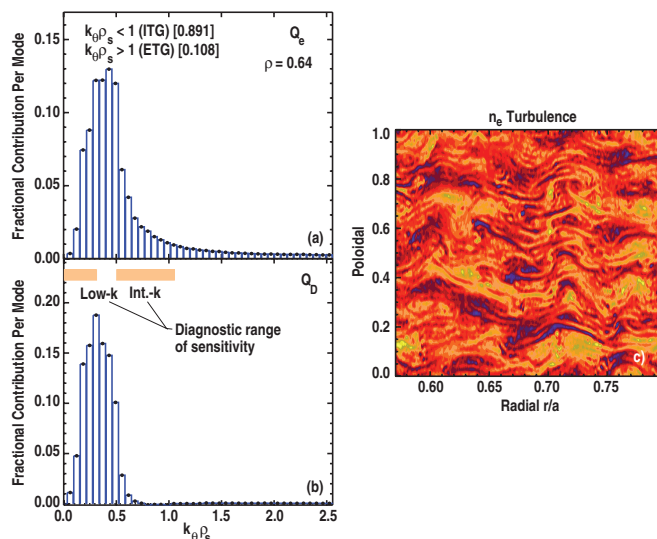


FIG. 11. (Color) Fractional contribution to (a) electron heat flux and (b) deuterium ion heat flux per mode from local flux tube GYRO simulations at $\rho=0.64$. The range in $k_{\theta}\rho_s$ for low and intermediate- k fluctuation measurements is indicated by the shaded region. (c) Simulated electron density turbulence showing long radial eddies.

global simulation and power balance analysis are also in good agreement in this region for the electron thermal diffusivity while the global simulation diffusivity is about half the power balance diffusivity for the ions. It should be noted that this is much better agreement than found for the case with ECH at $\rho_{ECH}=0.5$ where local GYRO analysis of the ion and electron power flowing through the flux surface at $\rho=0.5$ was over predicted by factors of ~ 15 and ~ 8 , respectively, compared to power balance analysis and by a factor of ~ 6 for both electrons and ions in global simulations. Stabilization by $E \times B$ flow shear is small in these low rotation discharges without NBI and thus inclusion of this process is not effective in helping to reduce the simulated heat flux for the case at $\rho_{ECH}=0.5$. A significant decrease in gradients is required to improve the agreement at $\rho=0.5$, a reduction of a/L_{Ti} and a/L_{Te} by $\sim 25\%$, and a/L_{ne} by $\sim 50\%$. It remains unresolved as to why there is much better agreement between simulation and power balance analysis at $\rho=0.6$ compared to 0.5 but uncertainties in profile measurements is not a likely candidate. It should also be noted that $\sim 30\%$ of the total ion transport is carried by carbon ions, the dominant impurity, at both $\rho=0.5$ and 0.6.

Thermal diffusivity and heat flux from local GYRO simulations are dominated by low- k turbulence for the high a/L_{Te} case at $\rho=0.64$ (Fig. 11). The fractional contribution to heat flux peaks at $k_{\theta}\rho_s \sim 0.3-0.4$ for both electrons and ions. Even at these low wave numbers the modes dominantly contributing to the electron heat flux are calculated to propagate in the electron diamagnetic direction. About 11% of the total electron heat flux is due to fluctuations with $k_{\theta}\rho_s > 1$. The region over which low and intermediate- k measurements were made is indicated in Fig. 11 and shows that the low- k measurements are most important for capturing modes with the dominant contribution to heat flux while the intermediate- k measurements carry less, but not negligible,

weight in this regard and offer additional useful points of comparison to simulations. Simulated density fluctuations show turbulent eddies with long correlation lengths in the radial direction [Fig. 11(c)].

Simulated cross-phase angles between density and temperature fluctuations at low- k for the high a/L_{Te} case were in good agreement with the sign and spectral trend measured. The simulated spectral response was larger than zero for frequencies below ~ 30 kHz. The simulated magnitude was about half that measured for frequencies 10–20 kHz with $47^\circ \pm 11^\circ$ from GYRO simulations compared to $98^\circ \pm 7^\circ$ measured. It is interesting to note that in a different experiment cross-phase measurements indicated negative phase values for ITG dominated plasmas.¹⁷

Comparison of the measured change in turbulence between the high and low a/L_{Te} conditions with simulations requires a simulation of both conditions. The low a/L_{Te} case has proven to be very challenging. The measured profiles for this case are near the marginality condition. Using these profiles as input to a local flux tube simulation, the turbulence is calculated to be in the zonal flow dominated regime^{18,19} for both the four and six gyrotron cases at $\rho \geq 0.6$. These simulations show long wavelength modes that retain a linear structure and saturate at very small amplitude. This condition persists even when including zonal flow damping by ion-ion collisions. For these cases the local model assumption that the radial correlation length of the turbulence is small compared to the spatial scale over which the drive term, a/L_{Te} , varies is no longer valid. Thus indicating that a global rather than local analysis is required. Unfortunately, global simulations for this low a/L_{Te} case have so far been numerically unstable.

Given this difficulty with the low a/L_{Te} case, an alternate approach was employed where the measured profiles were used for the high a/L_{Te} case and then the drive term was reduced by the experimentally observed value, 30% at $\rho=0.64$, for the low a/L_{Te} case with all other profiles taken from the high a/L_{Te} case. This resulted in a local simulation with turbulence characteristics that were more physical, such as a peaked rather than flat wave number spectrum, finite transport levels, and finite radial correlation lengths. With this approach of reducing a/L_{Te} in the local simulations of the high a/L_{Te} case at $\rho=0.64$, GYRO simulations of the change in low- k temperature fluctuations agree well with the experimental measurements of the change in low- k turbulence as a/L_{Te} is modulated (Fig. 12). The relative change in fluctuation level from the simulations is shown in Fig. 12(b) for $k_\theta \rho_s \leq 2.5$, where the change is obtained from the two simulations in Fig. 12(a). A synthetic CECE diagnostic module²⁰ was developed for GYRO which takes into account the viewing geometry and wave number sensitivity of the system. When applied to the simulations for high and low a/L_{Te} the simulation values of \tilde{T}_e/T_e are reduced by about 40% making the synthetic module a necessary component in the quantitative comparison process. With the module filtering applied the simulation of \tilde{T}_e/T_e is 1.6% and 0.75% for the high and low a/L_{Te} cases, respectively, about a factor of 2 larger than the measurements (Fig. 8). Since the impact of

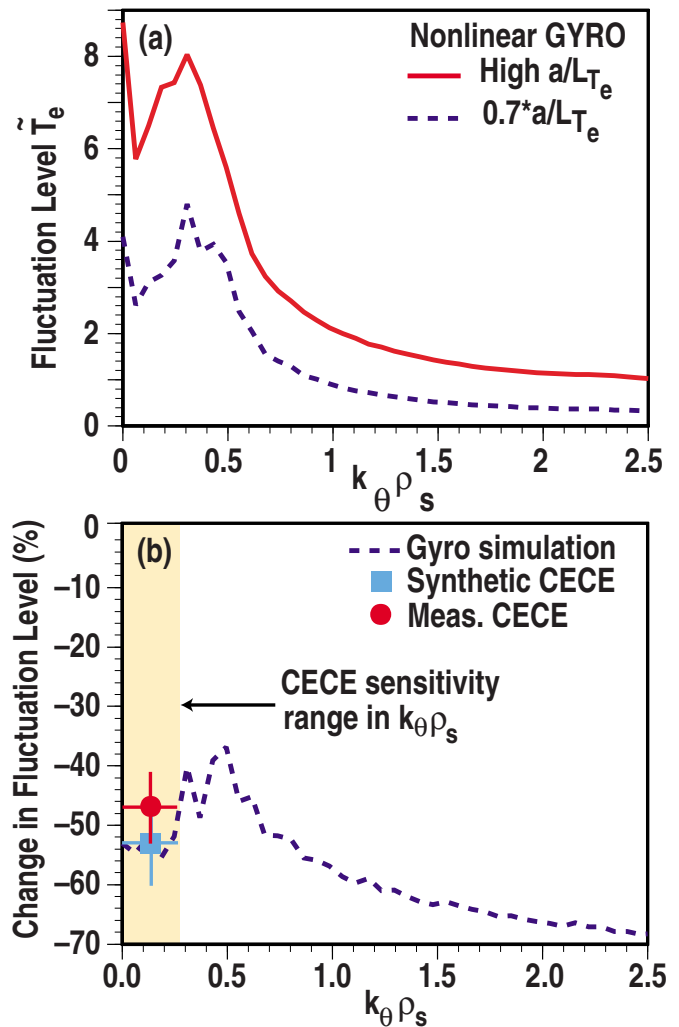


FIG. 12. (Color online) Simulated electron temperature fluctuation levels (a) for the high drive term phase (solid) and for a low drive term taken to be 30% below the high drive term (dashed) for the six gyrotron case at $\rho=0.64$. (b) Change in fluctuation level simulated (dashed), simulated with application of a synthetic CECE diagnostic module (square), and measured with the CECE system (circle). The shaded region indicates the range in $k_\theta \rho_s$ for the CECE system.

the synthetic module was comparable for the high and low a/L_{Te} cases, there is little difference between the relative change in temperature fluctuations with and without the module filtering [Fig. 12(b)]. The simulated change in temperature fluctuations, -57% , is within estimated uncertainties of the measured change, -47% . In contrast to the agreement between the measured change in low- k \tilde{T}_e/T_e and the calculated change, it should be noted that the simulation of the change in density fluctuations at intermediate- k did not agree with the experimental trend; the measured reversal in the turbulence response to a/L_{Te} changes for six gyrotrons was not reproduced by the simulation. One should recall that the rapid spatial changes in drive term measured, from an increase just inside the peak inside ECH deposition to a large decrease a few centimeters further out where the turbulence growth rate is significantly reduced, indicate that a global GYRO analysis is needed. This result remains interesting

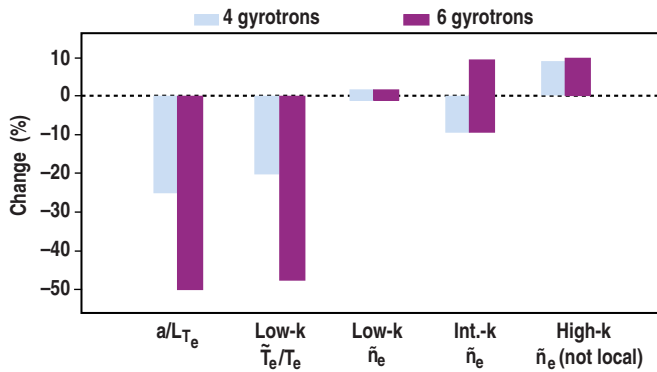


FIG. 13. (Color online) Summary of the experimental results for changes in drive term a/L_{Te} and range in measured turbulence responses for four gyrotrons and six gyrotrons.

and not understood at present. Additional comparisons between simulation and turbulence response are ongoing and the results are planned for a future publication.

VI. SUMMARY AND CONCLUSIONS

ECH was alternately applied at two spatial locations in the plasma centered near $\rho=0.6$ to modulate the local value of the normalized inverse temperature gradient scale length a/L_{Te} , a turbulence drive term. This produced low and high a/L_{Te} phases in 25 ms intervals throughout the flattop current phase of a low collisionality L-mode, inner wall limited discharge. Two power levels were studied: four gyrotrons and, later in the same discharges, six gyrotrons giving total average input powers of ~ 1.5 and 2 MW, respectively. The turbulence responses to changes in drive term were measured in low- k (\tilde{n} and \tilde{T}_e) and intermediate and high- k regimes (\tilde{n}) (Fig. 13). With four gyrotrons the drive term was reduced by up to 25% with respect to the high a/L_{Te} phase, which produced a comparable reduction in low- k temperature fluctuations. No change in low- k density fluctuations were observed while intermediate- k fluctuations were reduced by up to 9%. Further reductions in a/L_{Te} with six gyrotrons resulted in a very interesting reversal in intermediate- k density turbulence response, where the turbulence level increased up to 10% when a/L_{Te} was reduced up to 50%. With six gyrotrons the low a/L_{Te} phase was calculated by linear analysis to be near the marginal stability condition for TEMs, which may be related to the reversed turbulence response observed for intermediate- k density fluctuations. The change in low- k temperature fluctuations was of the same sign and magnitude as the change in local drive term.

Initial comparisons between simulations with the nonlinear gyrokinetic turbulence code GYRO and power balance and turbulence measurements were performed. Global simulations of electron thermal diffusivity were within 10% or less of power balance analysis with ONETWO and local simulations were within 40% or less for $\rho \geq 0.6$ for the high a/L_{Te} case with six gyrotrons. Simulations of the ion thermal diffusivity were about half the power balance analysis values. The simulations indicated that the electron and ion thermal diffusivities were dominated by low- k turbulence with the dominant contributions peaking at $k_{\theta}\rho_s=0.3-0.4$. Local flux

tube simulations of temperature fluctuations for high and low drive term levels with six gyrotrons were consistent with measured changes in low- k temperature fluctuations. However, a global analysis is required because the radial correlation length of the turbulence is no longer short compared to the spatial scale of the change in drive term for the low a/L_{Te} phase. Global analysis of the low a/L_{Te} phase has been challenging due to numerical instabilities that must be overcome before progress can be made for this case. Overall these experiments have produced a rich set of data for which detailed comparisons with simulations from nonlinear gyrokinetic turbulence codes such as GYRO can be carried out to make progress on code validation studies.

ACKNOWLEDGMENTS

This work was supported by the U.S. Department of Energy under Grant Nos. DE-FC02-04ER54698, DE-FG02-07ER54917, DE-FG03-08ER54984, DE-AC05-06OR23100, DE-FG03-97ER54415, DE-FG02-89ER53296, and DE-FG03-08ER54999 and utilized resources of the National Center for Computational Sciences at Oak Ridge National Laboratory under Grant No. DE-AC05-00OR22725. The authors gratefully acknowledge the contributions of the DIII-D physics, operations, and RF groups in the execution of the experiments described.

- ¹M. Shimada, D. J. Campbell, V. Mukhovatov, M. Fujiwara, N. Kirneva, K. Lackner, M. Nagami, V. D. Pustovitov, N. Uckan, J. Wesley, N. Asakura, A. E. Costley, A. J. H. Donné, E. J. Doyle, A. Fasoli, C. Gormezano, Y. Gribov, O. Gruber, T. C. Hender, W. Houlberg, S. Ide, Y. Kamada, A. Leonard, B. Lipschultz, A. Loarte, K. Miyamoto, V. Mukhovatov, T. H. Osborne, A. Polevoi, and A. C. C. Sips, *Nucl. Fusion* **47**, S1 (2007).
- ²J. L. Luxon, *Nucl. Fusion* **42**, 614 (2002).
- ³J. Candy and R. Waltz, *J. Comput. Phys.* **186**, 545 (2003).
- ⁴W. A. Peebles, *Bull. Am. Phys. Soc.* **49**, 247 (2004).
- ⁵T. L. Rhodes, W. A. Peebles, M. A. Van Zeeland, J. S. deGrassie, R. V. Bravenec, K. H. Burrell, J. C. DeBoo, J. Lohr, C. C. Petty, X. V. Nguyen, E. J. Doyle, C. M. Greenfield, L. Zeng, and G. Wang, *Phys. Plasmas* **14**, 056117 (2007).
- ⁶H. Hutchinson, R. Boivin, F. Bombardia, P. Bonoli, S. Fairfax, C. Fiore, J. Goetz, S. Golovato, R. Granetz, M. Greenwald, S. Hubbard, J. Irby, B. LaBombard, B. Lipschultz, E. Marmor, G. McCracken, M. Porkolab, J. Rice, J. Snipes, Y. Takase, J. Terry, S. Wolfe, C. Christensen, D. Garnier, M. Graf, T. Hsu, T. Luke, M. May, A. Nemczewski, G. Tinio, J. Schachter, and J. Urbahn, *Phys. Plasmas* **1**, 1511 (1994).
- ⁷D. R. Ernst, N. Basse, W. Dorland, C. L. Fiore, L. Lin, A. Long, M. Porkolab, K. Zeller, and K. Zhurovich, Proceedings of the 21st International Atomic Energy Agency Fusion Energy Conference, Chengdu, China, 2006, IAEA-CN-149/TH/1-3. Available as http://www-pub.iaea.org/MTCD/Meetings/FEC2006/th_1-3.pdf.
- ⁸G. M. Staebler, J. E. Kinsey, and R. E. Waltz, *Phys. Plasmas* **14**, 055909 (2007).
- ⁹H. E. St John, T. S. Taylor, Y. R. Lin-Liu, and A. D. Turnbull, *Plasma Phys. Controlled Nucl. Fusion Res.* **3**, 603 (1994).
- ¹⁰M. E. Austin and J. Lohr, *Rev. Sci. Instrum.* **74**, 1457 (2003).
- ¹¹L. Schmitz, G. Wang, J. C. Hillesheim, T. L. Rhodes, W. A. Peebles, A. E. White, L. Zeng, T. A. Carter, and W. M. Solomon, *Rev. Sci. Instrum.* **79**, 10F113 (2008).
- ¹²G. R. McKee, R. J. Fonck, D. K. Gupta, D. J. Schlossberg, M. W. Shafer, R. L. Boivin, and W. M. Solomon, *Plasma Fusion Res.* **2**, S1025 (2007).
- ¹³A. E. White, L. Schmitz, W. A. Peebles, T. A. Carter, T. L. Rhodes, E. J. Doyle, P. A. Gourdain, J. C. Hillesheim, G. Wang, C. Holland, G. R. Tynan, M. E. Austin, G. R. McKee, M. W. Shafer, K. H. Burrell, J. Candy, J. C. DeBoo, R. Prater, G. M. Staebler, R. E. Waltz, and M. A. Makowski, *Rev. Sci. Instrum.* **79**, 103505 (2008).
- ¹⁴J. C. Hillesheim, W. A. Peebles, T. L. Rhodes, L. Schmitz, T. A. Carter, P. A. Gourdain, and G. Wang, *Rev. Sci. Instrum.* **80**, 083507 (2009).

- ¹⁵T. L. Rhodes, W. A. Peebles and X. Nguyen, *Rev. Sci. Instrum.* **77**, 10E922 (2006).
- ¹⁶R. E. Waltz, J. Candy, and M. Fahey, *Phys. Plasmas* **14**, 056116 (2007).
- ¹⁷A. E. White, W. A. Peebles, T. L. Rhodes, C. H. Holland, G. Wang, L. Schmitz, T. A. Carter, J. C. Hillesheim, E. J. Doyle, L. Zeng, G. R. McKee, G. M. Staebler, R. E. Waltz, J. C. DeBoo, C. C. Petty, and K. H. Burrell, *Phys. Plasmas* **17**, 056103 (2010).
- ¹⁸A. M. Dimits, G. Bateman, M. A. Beer, B. I. Cohen, W. Dorland, G. W. Hammett, C. Kim, J. E. Kinsey, M. Kotschenreuther, A. H. Dritz, L. L. Lao, J. Mandrekas, W. M. Nevins, S. E. Parker, A. J. Redd, D. E. Shumaker, R. Sydora, and J. Weiland, *Phys. Plasmas* **7**, 969 (2000).
- ¹⁹D. R. Mikkelsen and W. Dorland, *Phys. Rev. Lett.* **101**, 135003 (2008).
- ²⁰C. Holland, A. E. White, G. R. McKee, M. W. Shafer, J. Candy, R. E. Waltz, L. Schmitz, and G. R. Tynan, *Phys. Plasmas* **16**, 052301 (2009).